Journal of Ethnopharmacology 274 (2021) 114032

Contents lists available at ScienceDirect

Journal of Ethnopharmacology

journal homepage: www.elsevier.com/locate/jethpharm

Green tea infusion prevents diabetic nephropathy aggravation in recent-onset type 1 diabetes regardless of glycemic control

Luiz Carlos Maia Ladeira [a,*], Eliziária Cardoso dos Santos [b], Talita Amorim Santos [a], Janaina da Silva [a,c], Graziela Domingues de Almeida Lima [a], Mariana Machado-Neves [a], Renê Chagas da Silva [d], Mariella Bontempo Freitas [e], Izabel Regina dos Santos Costa Maldonado [a]

[a] Departamento de Biologia Geral, Universidade Federal de Viçosa, Viçosa, Minas Gerais, Brazil
[b] Escola de Medicina da Universidade Federal do Vale do Jequitinhonha e Mucuri, Diamantina, Minas Gerais, Brazil
[c] Institut de Recherche en Santé, Environnement et Travail, Université de Rennes, Rennes, France
[d] Departamento de Física, Universidade Federal de Viçosa, Viçosa, Minas Gerais, Brazil
[e] Departamento de Biologia Animal, Universidade Federal de Viçosa, Minas Gerais, Brazil

ARTICLE INFO

Keywords:
Diabetic nephropathy
Type 1 diabetes
Recent-onset diabetes
Diabetic kidney disease
Green tea

ABSTRACT

Ethnopharmacological relevance: Green tea, traditionally used as antidiabetic medicine, positively affects the diabetic nephropathy. It was assumed that these beneficial effects were due to the hypoglycemiant capacity of the tea, wich reduces the glycemic overload and, consequently, the advanced glycation end products rate and oxidative damage. However, these results are still controversial, since tea is not always able to exert a hypoglycemic action, as demonstrated by previous studies.

Aim: Investigate if green tea infusion can generate positive outcomes for the kidney independently of glycemic control, using a model of severe type 1 diabetes.

Abbreviation: 67LR, 67kDa laminin receptor; ABTS, 2,2'-Azinobis-[3-ethylbenzthiazoline-6-sulfonic acid]; NOS1, Nitric Oxide Synthase 1; AGE/RAGE, advanced glycated end-products and its receptor; AKT, protein kinase B; AMPK, 5'-AMP-activated protein kinase; AO, acridine Orange; APC, APC Regulator Of WNT Signaling Pathway; ATP, adenosine triphosphate; BAX, BCL2 Associated X; BCL2, BCL2 Apoptosis Regulator; BID, BH3 Interacting Domain Death Agonist; BW, body weight; Ca, calcium; CaCl, calcium chloride; CASP3, Caspase 3; CASP8, Caspase 8; CASP9, Caspase 9; CAT, catalase; CAV1, Caveolin 1; CCL2, C-C Motif Chemokine Ligand 2; CDK2, Cyclin Dependent Kinase 2; CDKN1A, Cyclin Dependent Kinase Inhibitor 1; CIAPIN1, Cytokine Induced Apoptosis Inhibitor 1; c-kit, proto-oncogene c-kit; Cl, chlorine; CPI, compound-protein interactions; CTNNB1, Catenin Beta 1; Ctrl, control group; DB02077, L-N(omega)-nitroarginine-(4R)-amino-L-proline amide (NOS3); DB08019, DB08018 and NOS3- Nitric Oxide Synthase 3; DKG, diacylglycerol kinase; DN, Diabetic nephropathy; EGCG, epigallocatechin gallate; FGF, fibroblast growth fator; FGFR, fibroblast growth factor receptor; FOS, Fos Proto-Oncogene; FRAP, ferric reducing antioxidant power; GSK3β, glycogen synthase kinase-3 β; GST, glutathione S-transferase; GTI, Green tea infusion; H_2O_2, hydrogen peroxide; H6PD, Hexose-6-Phosphate Dehydrogenase/Glucose 1-Dehydrogenase; HIF1A, Hypoxia Inducible Factor 1 Subunit Alpha; HMG1, high-mobility group box 1; HSP90AA1, Heat Shock Protein 90 Alpha Family Class A Member 1; i.p., intraperitoneal; IL6, Interleukin 6; IL8, Interleukin 8; JUN, Jun Proto-Oncogene; K, potassium; KCl, potassium chloride; KW, kidney weight; MAP2K1, Mitogen-Activated Protein Kinase Kinase 1; MAPK1, Mitogen-Activated Protein Kinase 1; MAPK3, Mitogen-Activated Protein Kinase 3; MAPK8, Mitogen-Activated Protein Kinase 8; MAPKAPK5, MAPK Activated Protein Kinase 5; Mg, magnesium; MgCl, magnesium chloride; MLH1, MutL Homolog 1; mTOR, mammalian target of rapamycin; MTRR, 5-Methyltetrahydrofolate-Homocysteine Methyltransferase Reductase; Na, sodium; NaCl, sodium chloride; NADPH, reduced nicotinamide adenine dinucleotide phosphate; NDOR1, NADPH-dependent diflavin reductase; NfκB, nuclear factor κ B; NO_2^-/NO_3^-, nitric oxide; NOS2, Nitric Oxide Synthase 2; NR1H4, Nuclear Receptor Subfamily 1 Group H Member 4; O_2, oxygen; O^-_2, superoxide; PARP1, Poly(ADP-Ribose) Polymerase 1; PDGF, platelet-derived growth fator; PGD, Phosphogluconate Dehydrogenase; PGLS, 6-Phosphogluconolactonase; PI, propidium iodide; PI3K, phosphoinositide 3-kinase; PIN1, Peptidylprolyl Cis/Trans Isomerase, NIMA-Interacting 1; PKC-β, protein kinase C beta; POR, Cytochrome P450 Oxidoreductase; PPI, Protein-Protein Interactome; RPIA, Ribose 5-Phosphate Isomerase A; RSI, renal somatic index; SCF, stem cell fator; SD, standard deviation; SGLT1, sodium-dependent glucose transporter 1; SGLT2, sodium-dependent glucose transporter 2; SOD, superoxide dismutase; SOES, Specific Organ Expression Score; STAT3, Signal transducer and activator of transcription 3; STZ, streptozotocin; TCA, Trichloroacetic acid; TCF7L2, Transcription Factor 7 Like 2; TE, Trolox equivalente; TGF-β, transforming growth factor-beta; TLR4, toll-like receptor 4; TP53, tumor protein 53; TRIF, TIR domain-containing adaptor-inducing Interferon- β; TYW1, TRNA-YW Synthesizing Protein 1 Homolog; UBC, Ubiquitin C.

* Corresponding author. Departamento de Biologia Geral, Universidade Federal de Viçosa, Av. P.H. Rolfs, s/n, Campus Universitário, Viçosa, 36570-900, Minas Gerais, Brazil.

E-mail addresses: luizmaialadeira@gmail.com, luiz.ladeira@ufv.br (L.C.M. Ladeira), lisa.famed@gmail.com (E.C. dos Santos), taliamorims@gmail.com (T.A. Santos), janaina.silva2@ufv.br (J. da Silva), graziela.gdal@gmail.com (G.D.A. Lima), machadonevesm@gmail.com (M. Machado-Neves), rene.silva@ufv.br (R.C. da Silva), mariellafreitas@gmail.com (M.B. Freitas), irscmaldonado@gmail.com (I.R.S.C. Maldonado).

https://doi.org/10.1016/j.jep.2021.114032
Received 20 January 2021; Received in revised form 11 March 2021; Accepted 12 March 2021
Available online 15 March 2021

Material and methods: We treated streptozotocin type 1 diabetic young rats with 100 mg/kg of green tea, daily, for 42 days, and evaluated the serum and tissue markers for stress and function. We also analyzed the ion dynamics in the organ and the morphological alterations promoted by diabetes and green tea treatment. Besides, we analyzed, by an *in silico* approach, the interactions of the green tea main catechins with the proteins expressed in the kidney.
Results: Our findings reveal that the components of green tea can interact with the proteins participating in cell signaling pathways that regulate energy metabolism, including glucose and glycogen synthesis, glucose reabsorption, hypoxia management, and cell death by apoptosis. Such interaction reduces glycogen accumulation in the organ, and protects the DNA. These results also reflect in a preserved glomerulus morphology, with improvement in pathological features, and suggesting a prevention of kidney function impairment.
Conclusion: Our results show that such benefits are achieved regardless of the blood glucose status, and are not dependent on the reduction of hyperglycemia.

1. Introduction

Diabetic nephropathy (DN) affects 25%–35% of type 1 and 2 diabetic patients (Herman-Edelstein and Doi, 2016) and accounts for about 45% of the patients with end-stage renal disease (Su et al., 2020). It progresses from the increase in the glomerular filtration rate to the total failure of the kidneys, passing through alterations that indicate damage to the renal glomeruli and tubules, albuminuria, mesangial expansion, fibrosis, and vascular damage (Gilbert, 2017; Herman-Edelstein and Doi, 2016). In addition, glycogenic accumulation in the proximal tubules is a common feature in DN, and one of the earliest signals of metabolic impairment in the organ (Gilbert, 2017; Haraguchi et al., 2020). Such damage can progress in renal cells to pre-neoplastic lesions which, if left untreated, may progress to renal cancer (Ribback et al., 2015).

Green tea (*Camellia sinensis* (L.) Kuntze (Theaceae)), popularly used as a traditional medicine, in the form of infusion, for many porpoises including hyperglycaemia (Barkaoui et al., 2017; Chopade et al., 2008; Fallah Huseini et al., 2006; Rachid et al., 2012), is known to exert positive effects in diabetes management (Meng et al., 2019; Mohabbulla Mohib et al., 2016). Recent studies have shed light on the mechanisms through which tea catechins positively affect the DN, with special focus on the podocyte (Hayashi et al., 2020), through the activation of the 67 kDa laminin receptor (67LR) by the epigallocatechin gallate (EGCG), the main polyphenol in green tea. Such interaction results in the preservation of podocyte morphology and the glomerular filtration function, suggesting an improvement in DN. However, tubular alterations, with glycogen accumulation, and aberrant activation of the advanced glycated end-products and its receptor (AGE/RAGE system), wich affec the cellular renovation and survival, are considered the primary cause of proximal tubular function disruptment (Haraguchi et al., 2020). This, in turn, can affect glomerular function by the proximal tubule/glomerulus feedback system, thus leading to glomerular damage and contributing to the progression of DN.

It was assumed that the beneficial effects of the green tea on proximal tubules were due to the tea's hypoglycemiant capacity (Renno et al., 2008; Yokozawa et al., 2012), which reduces the glycemic overload and, consequently, the AGE rate and oxidative damage. However, tea effects in diabetic human subjects are still controversial. The first double-blind controlled trial treating diabetic patients (100% type 2 diabetic) with green tea polyphenols describes a reduction in podocyte apoptosis and an improvement of kidney function by reducing microalbuminuria (Borges et al., 2016). Another double-blind controlled trial conducted with diabetic adult patients (70.3% type 1 diabetic) failed to achieve glycemic control or improve renal function after green tea consumption (Vaz et al., 2018). On the other hand, tea catechins can inhibit gluconeogenesis by activating the 5′AMP-activated protein kinase (AMPK) (Collins et al., 2007), possibly reducing glycogenic nephrosis. Also, EGCG can activate the protein kinase B (AKT) pathway, thus enhancing cell survival and preserving nephron morphology (Hayashi et al., 2020). These effects may contribute to the prevention of DN development in recent-onset diabetes (Haraguchi et al., 2020).

In a previous study, we demonstrated that the infusion of green tea was not able to prevent hyperglycemia in animals with experimental type 1 diabetes induced by streptozotocin (STZ) in young male Wistar rats (Ladeira et al., 2020a). Therefore, in the same model, we tested the hypothesis that the beneficial effects of tea in DN go beyond glycemic control. In this way, we investigated the effects of green tea infusion treatment on diabetic kidney disease in recent-onset type 1 diabetic young rats. Also, we used bioinformatics tools to explore tea catechin interaction in signaling pathways in the kidney.

2. Materials and methods

2.1. Animals and ethics

Eighteen male Wistar rats (30 days old; 82.52 ± 10.83 g) were

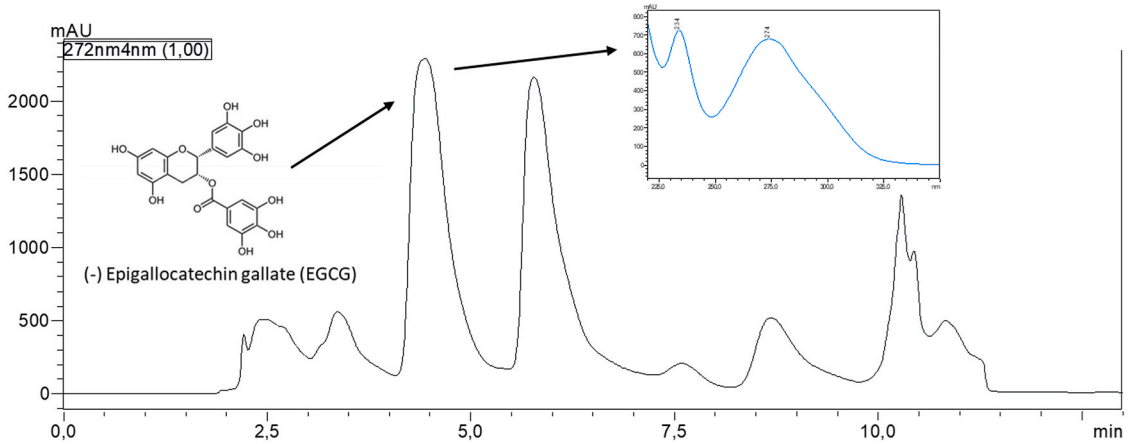

Fig. 1. Chromatogram of the green tea infusion (*Camellia sinensis*). In detail: UV spectrum of the major compound (Epigallocatechin gallate).

housed, two per cage, in polypropylene cages with autoclaved sawdust as cage bed, under controlled conditions of temperature (22 ± 2 °C) and light-dark cycles (12/12 h), and received food (Presence Alimentos, Paulínea, SP, Brazil) and water *ad libitum*. The use of animals in the research was approved by the Ethics Committee of Animal Use of the Federal University of Viçosa (CEUA/UFV – protocol number 53/2018).

2.2. Green tea infusion preparation and analysis

Green tea (*Camellia sinensis*) leaves were obtained from Leão® - Food and Beverages (Coca-Cola Company®, lot LO159), and prepared as infusion, to mimic the way it is normally consumed by humans. The infusion was prepared mixing the leaves with warm distilled water (1:40 w/v, 80 °C) (Perva-Uzunalić et al., 2006). The mixture remained infused for 20 min on a magnetic stirrer. Then, it was filtered through a 0.45 μm porous filter, frozen at −80 °C and lyophilized. The lyophilized samples were resuspended in distilled water at the moment of use.

The chromatographic profile, or fingerprint, was determined as described by Kim-Park et al. (Kim-Park et al., 2016), with some modifications. High-performance liquid chromatography (HPLC) (Prominence LC-20 A, Shimadzu, Kyoto, Japan), equipped with Diode Arrangement Detector (DAD), LC-20AD pump, SPD-M20A detector, CTO-20 A oven and LabSolutions software, was used to determine the EGCG content using a maximal absorption peaks at 272 nm. It was used a Vydac C18 (4.6 × 250 mm) column, at 30 °C, with a 5 μL injection volume. The mobile phase was composed of water and 2.0% acetic acid (1:1). The infusion lyophilized powder was suspended in methanol before analysis. The mobile phase flow rate was 1.0 mL/min and the run time was 15 min. The retention time of the main component, EGCG, was 4.5 min and the total amount of it was calculated using a standard curve (r^2 = 0.9967) developed under the same conditions using an EGCG chemical standard (≥98.0%, Sigma Aldrich Inc. - CAS Number 989-51-5. St. Louis, MO, USA). The EGCG content accounted for 19.38% of the total GTI content. The fingerprint is presented in Fig. 1.

Also, we determined the total phenolic content and antioxidant capacity as previously described (Ladeira et al., 2020a). GTI presented a total amount of phenolic components of 3.88 ± 2.49 mg gallic acid equivalent (GAE)/g GTI. The extract presented an antioxidant capacity of 3.26 ± 0.06 μMol Trolox equivalent (TE)/g GTI in the 2,2′-Azinobis-[3-ethylbenzthiazoline-6-sulfonic acid] (ABTS) assay and 46.38 ± 4.10 μMol FeSO4/g GTI in the ferric reducing antioxidant power (FRAP) assay.

2.3. Experimental design, euthanasia, and tissue collection

Twelve rats were randomly selected to integrate the diabetics groups. After 12 h fasting, diabetes was induced by a single intraperitoneal (i.p.) injection of streptozotocin (STZ) (Sigma Chemical Co., St, Louis, MO, USA) at a dosage of 60 mg/kg of body weight (BW) diluted in 0.01 M sodium citrate buffer, pH 4.5. The healthy control group (n = 6) received the buffer alone (i.p.) to simulate the injection stress. Fasting blood glucose levels were measured after 2 days using a glucometer (Accu-Chek® Performa, Roche LTDA. Jaguaré, SP, Brazil) in blood samples collected at the tail vein. All STZ-injected animals presented the fasting glycemia levels higher than 250 mg/dL and were included in the study. The diabetic rats were divided into two groups (n = 6, each). Therefore, the experiment consisted of three groups: the healthy control group (Ctrl, n = 6), which received water as a placebo; the diabetic control group (STZ, n = 6), which also received water; and the diabetic group treated with the green tea infusion (STZ + GTI, n = 6), wich received the GTI (100 mg/kg body weight). All treatments were administered daily, by gavage, for 42 days. The dosage was equivalent to 7 cups (200 mL) of tea, prepared according to the manufacturer instructions, mimicking a feasible human consumption dosage, considering survey data from the Asian population (Mineharu et al., 2011).

We monitored body weight and water consumption using a precision scale (BEL M503, e = 0.001 g, Piracicaba, SP, Brazil), and 12 h fasting blood glucose using test strips and a glucometer (Accu-Chek® Performa, Roche LTDA. Jaguaré, SP, Brazil), in blood samples from the tail vein.

After the experimental period, the animals were euthanized by deep anesthesia (sodium thiopental, 60 mg/kg i.p.) followed by cardiac puncture and exsanguination. The kidneys were removed and weighed. One kidney (right) of each animal was frozen in liquid nitrogen and stored at −80 °C for enzymatic analysis. The other one (left) was immersed in Karnovsky fixative solution for 24 h for histopathological analyses. The renal somatic index (RSI) was calculated using the ratio between the kidney weight (KW) and BW, where RSI = KW/BW × 100 (Sertorio et al., 2019).

2.4. Renal function markers

The blood samples collected by cardiac puncture during euthanasia were centrifuged at 4600 rpm, for 15 min, at 4 °C, and the serum was separated. Then, we performed the analysis for the quantification of urea and creatinine in the serum using biochemical kits (Bioclin Laboratories, Belo Horizonte, MG, Brazil) at the BS-200 equipment (Bioclin Laboratories, Belo Horizonte, MG, Brazil) following the manufacturer's instructions.

2.5. Antioxidant enzyme and nitric oxide analysis

The antioxidant enzyme analysis was performed with the supernatant obtained from 100 mg of frozen kidney tissue homogenized in ice-cold phosphate buffer (pH 7.0) and centrifuged at 12,000 rpm, for 10 min, at 4 °C. The activity of the superoxide dismutase enzyme (SOD) was assessed by the pyrogallol method based on the ability of this enzyme to catalyze the reaction of the superoxide (O^{-2}) and hydrogen peroxide (H_2O_2) (Dieterich et al., 2000). The glutathione S-transferase (GST) activity was measured according to the method of Habig et al. (1974), and calculated from the rate of NADPH oxidation. The activity of catalase (CAT) was determined by measuring the kinetics of hydrogen peroxide (H_2O_2) decomposition, as described by Aebi (1984). The nitric oxide (NO_2^- and NO_3^-) levels were quantified by the Griess method (Ricart-Jané et al., 2002). The values of enzyme activities were normalized by the total protein content, determined with the Folin–Ciocalteu method, according to Lowry et al. (1994).

2.6. Determination of Ca^{2+}, Na^+/K^+, Mg^{2+}, and total ATPase activities

The ATPase activity was determined following the procedure described by Al-Numair et al. (2015). Briefly, 100 mg of kidney fragments were homogenized in Tris-HCl buffer (0.1 M, pH 7.4) and centrifuged at 12,000 rpm, for 10 min, at 5 °C. The supernatant was used for the determination of the ATPase activity using NaCl, KCl, MgCl, and CaCl solutions at 0.1 M. ATP solution (0.1 M) was used as a substrate to generate free phosphate by the ATPases. The reaction was interrupted with a cold solution of 10% TCA and centrifuged at 6000 rpm, for 10 min. The supernatant was used to determine the inorganic phosphorus content by the Fiske and Subbarow method (Fiske and Subbarow, 1925). The ATPase activities were expressed as μMol of inorganic phosphorus/min mg of protein.

2.7. Chemical elements analysis

The proportion of chemical elements in the renal cortex was assessed per area in fragments of frozen kidney, as already described (Ladeira et al., 2020b). We measured the proportion of sodium (Na), magnesium (Mg), chlorine (Cl), potassium (K), and calcium (Ca). The fragments were dried at 60 °C, for 96 h, coated with carbon (Quorum Q150 T, East Grinstead, West Sussex, England, UK), and analyzed in a scanning electron microscope (JEOL, JSM-6010LA), with a Silicon Drift type X-ray detector system. The analysis was performed in an area of 250

Table 1
Blood Glucose, biometric parameters and water consumption of male Wistar diabetic rats treated or not with green tea infusion and a healthy control group.

	Ctrl	STZ	STZ + GTI
Blood Glucose (mg/dL)	85.38 ± 7.53	475.00 ± 33.14*	542.80 ± 42.20#
Initial body weight (g)	84.26 ± 14.97	81.27 ± 9.46	81.75 ± 7.57
Final body weight (g)	288.10 ± 44.16	93.08 ± 23.42*	99.75 ± 13.04
Body weight gain (g)	203.80 ± 30.81	11.82 ± 21.87*	18.00 ± 16.18
Kidney weight (g)	0.98 ± 0.07	0.78 ± 0.18#	0.86 ± 0.08
Renal somatic index (%)	0.34 ± 0.05	0.84 ± 0.13*	0.87 ± 0.10
Initial water consumption (mL/day)	44.45 ± 10.02	44.48 ± 9.87	41.78 ± 11.16
Final water consumption (mL/day)	39.25 ± 6.13	118.8 ± 17.45*	139.8 ± 10.26#

Mean ± SD. Data were compared by Student *t*-test (Ctrl vs STZ; STZ vs STZ + GTI) considering statistical differences when $P \leq 0.05$. Asterisk (*) indicates difference with $P < 0.0001$, and the hash (#) indicates different means with $P < 0.05$. (n = 6 animals/group).

μm^2, using an accelerating voltage of 20 kV and a working distance of 10 mm. The results were expressed as a mean value of the proportions between the elements present in the samples.

2.8. Histopathological and stereological analysis and assessment of DNA damage

The fragments fixed in Karnovsky solution were then dehydrated in a crescent ethanol series and embedded in Historesin® (Leica, Nussloch, Germany). A rotary microtome (RM 2255, Leica Biosystems, Nussloch, Germany) was used to cut the material into histological sections of 3 μm thickness. Then, the section was mounted in glass slides and reacted with periodic acid and Schiff reagent (PAS). Next, it was counterstained with hematoxylin for histopathological and stereological evaluation. The analysis was carried out as previously described by Sertorio et al. (2019). Also, slices stained with Toluidine Blue – Sodium borate 1% were used for the qualitative analysis of the glomeruli morphopathological features. We analyzed 40 glomeruli, randomly photographed, per experimental animal.

DNA damage was evaluated in sections of the kidney cortex stained with acridine orange (AO; green) and propidium iodide (PI; red) (Bernas et al., 2005; Suzuki et al., 1997). This fluorescent stain allows to evaluate the DNA damage, as damaged DNA presents red color, marked with PI, while integral DNA is marked in green by the AO (Dias et al., 2019). The digital images were captured using a photomicroscope (Olympus AX 70 TRF, Tokyo, Japan) and analyzed with Image-Pro Plus® 4.5 (Media Cybernetics, Silver Spring, MD) software, according to Lima et al. (2018).

2.9. Statistical analysis

All the results were submitted to the Shapiro-Wilk test to assess normality. The data expressed as percentages were transformed by angular transformation before the analysis. The results were expressed as mean ± standard deviation (mean ± SD) and analyzed using unpaired *t*-test, when the variances were equal (by *F* test), while the unpaired *t*-test with Welch's correction was used for data with unequal variances (Ctrl vs STZ; STZ vs STZ + GTI). The non-parametric data were compared with the Mann-Whitney test. The correlation analysis was carried out following Pearson's correlation method, as the analyzed data were normally distributed. Statistical significance was established at $P \leq 0.05$.

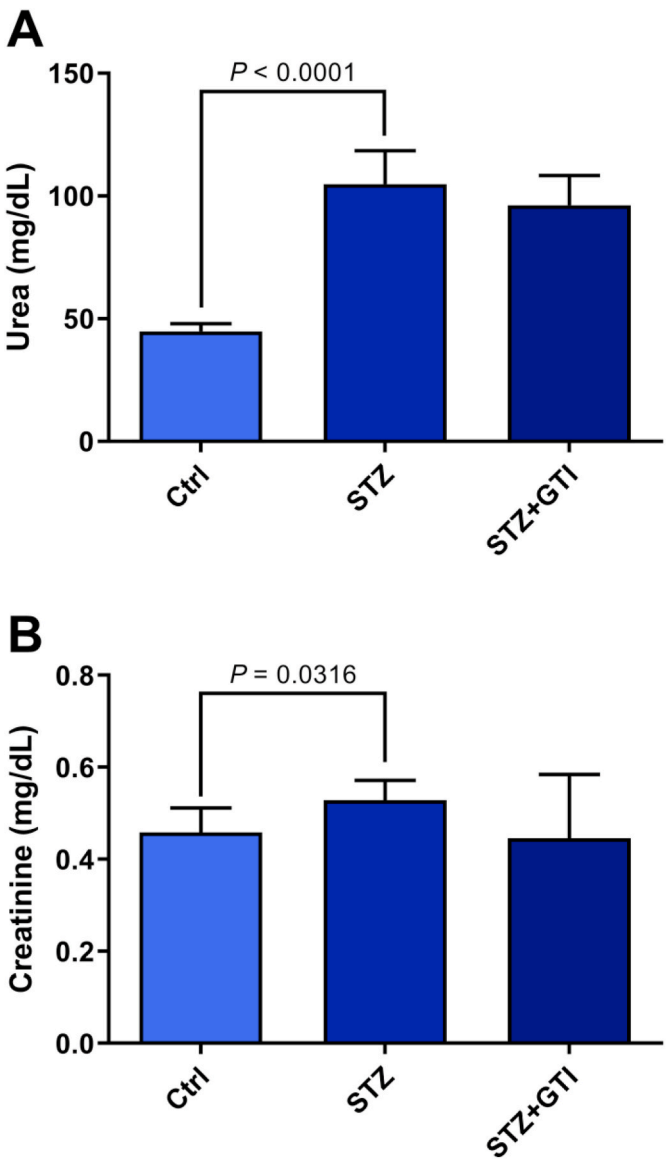

Fig. 2. Renal function markers of male Wistar diabetic rats treated or not with green tea infusion and a healthy control group. **A** – Urea (mg/dL). **B** – Creatinine (mg/dL). Mean ± SD. The statistical differences are indicated with lines with the *P*-value above or below them. Data were compared by Student *t*-test (Ctrl vs STZ; STZ vs STZ + GTI) considering statistical differences when $P \leq 0.05$. (n = 6 animals/group).

2.10. In silico pathway exploration

After the in vivo experiment, we explored, through an *in silico* approach, the interactions of green tea catechins with proteins, in search of possible signaling pathways involved in the generation of the observed effects. For such, we built and analyzed a network of interactions based on information from the STRING and STITCH databases (Szklarczyk et al., 2017, 2016).

A chemo-biology interactome network was built to elucidate the interactions between the tea compounds (catechins) and proteins expressed in the kidneys related to the positive effects found in the in vivo experiment with diabetic rats. A prospective evaluation of compound-protein interactions (CPI) was carried out with the STITCH v.5.0 database (http://stitch.embl.de/) (Szklarczyk et al., 2016). The CPI settings were performed according to (de Godoi et al., 2020). Briefly, the network downloaded from the database was limited to no more than 50 interactions, medium confidence score (0.400) and network depth

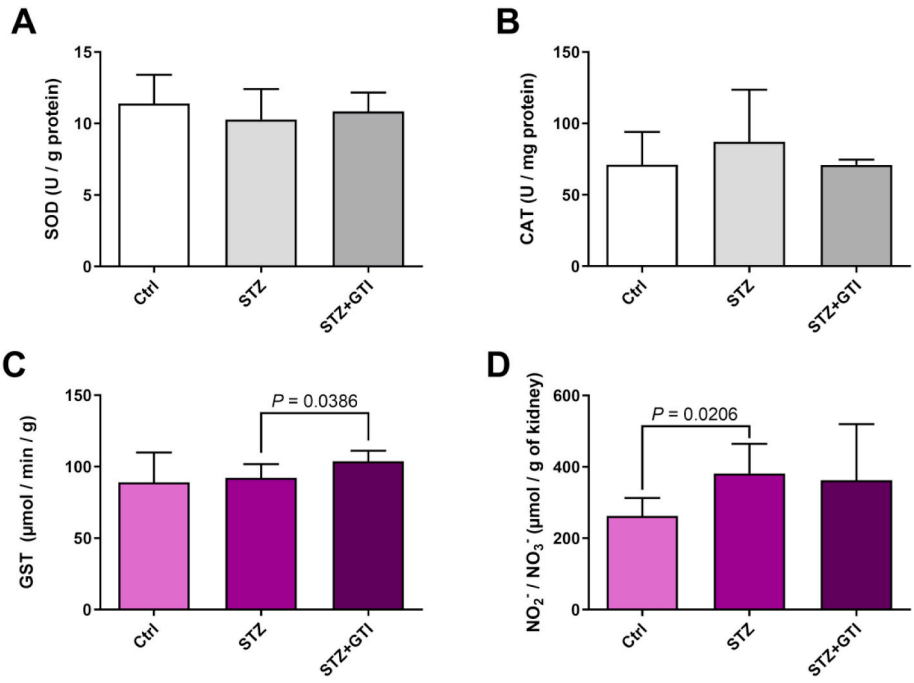

Fig. 3. Antioxidant enzymes and nitric oxide levels of male Wistar diabetic rats treated or not with green tea infusion and a healthy control group. **A** – Superoxide dismutase. **B** – Catalase. **C** – Glutathione S-Transferase. **D** – Nitric oxide. Mean ± SD. The statistical differences are indicated with lines with the *P*-value above or below them. Data were compared by Student *t*-test (Ctrl vs STZ; STZ vs STZ + GTI) considering statistical differences when $P \leq 0.05$. (n = 6 animals/group).

equal to 1. The following methods of predictions were activated: experiments, databases, co-expression, and predictions. The search was set to retrieve results for seven green tea catechins (Catechin, Catechin gallate, Epicatechin, Epicatechin Gallate, Epigallocatechin Gallate, Gallocatechin, and Gallocatechin Gallate), using the *Homo sapiens* species. All the catechins were imputed individually in the search, but only four (Catechin, Epicatechin, Epicatechin Gallate, and Epigallocatechin Gallate) retrieve results of interactions, thus generating four small CPI subnetworks (data not showed), wich were used in the posterior analysis.

The network analysis of four catechin-proteins was performed using Cytoscape v.3.8.0 (Shannon, 2003). The four subnetworks were merged using the merge tool with the union function of the software. Then, we "STRINGfy" the resultant network, through the STRING v.1.5.1 (Szklarczyk et al., 2017) to enable the protein interaction functions analysis. After that, we performed the Molecular Complex Detection analysis to detect clusters (i.e. densely connected regions) that may suggest functional protein complexes, with the MCODE v.1.6.1 app (Bader and Hogue, 2003). For such , the app was set up as already described(de Godoi et al., 2020). An MCODE score was calculated for each cluster. Additionally, the Reactome Pathways (Jassal et al., 2020) related to diabetic nephropathy pathogenesis were selected.

To identify proteins that could be considered as a key regulators of essential biological processes for the network, we performed a centrality analysis, using the CentiScaPe v.2.2 app (Scardoni et al., 2009) for Cytoscape. This app identifies the node (i.e. protein) that has a central position in the network by measuring the "betweenness" and "degree" of the node. Nodes with high betweenness and degree levels are named "bottlenecks" and are more likely to connect different clusters in the network (Yu et al., 2007).

The functional information about all the network proteins, including the tissue-specific expression score and the cellular location score, was accessed by the ClueGO v.2.5.7 and CluePedia v.1.5.7 apps (Bindea et al., 2013, 2009). The Specific Organ Expression Score (SOES) was accessed in this analysis and a filter to protein expression was used to apply the SOES to the PPI (Protein-Protein Interactome). Protein functions were accessed in the Human Gene database - GeneCards (http://www.genecards.org/) (Rebhan et al., 1998) and compared with the functions related to their effects in diabetic nephropathy described in the scientific literature.

3. Results

3.1. Experimental results

Diabetic animals presented classical signs of polydipsia (Table 1) and polyuria observed during the experiment (observed in the cage bed). The initial body weight was maintained throughout the experimental period in the animals of both diabetic groups, wich indicates a stagnation in the body weight gain, and a commitment of the body development by hyperglycemia, when compared to the healthy control group. Both diabetic groups remain severely hyperglycemic, and green tea infusion did not reduce blood glucose levels in the treated group.

The kidney weight was reduced in the diabetic groups when compared with the Ctrl group ($P < 0.0001$) and it was reflected in the kidney somatic index ($P < 0.0001$). In addition, this result may be related to the body development impairment due to hyperglycemia, as showed by the bodyweight reduced values. These data are presented in Table 1.

The serological analysis revealed that diabetes increased the serum levels of urea and the GTI did not modify this parameter (Fig. 2, A). Similarly, creatinine levels were also higher in the diabetic groups, compared to the healthy control without effect by GTI treatment (Fig. 2, B).

The GTI was capable of inducing a higher activity of GST enzyme (Fig. 3, C), and nitric oxide levels were increased in both diabetics groups, without any effect of the GTI treatment (Fig. 3, D). The activities of SOD and CAT in the kidney were not impacted by diabetes or GTI treatment in the kidney.

Fig. 4 shows the measurements of microelements and ions that participate in the filtration and reabsorption dynamics in the kidney. Although diabetes has not affected any of the elements analyzed (Fig. 4, A – F), green tea infusion altered Mg and Cl amounts compared to the STZ group (Fig. 4, B and D). Although all altered values (Mg and Cl)

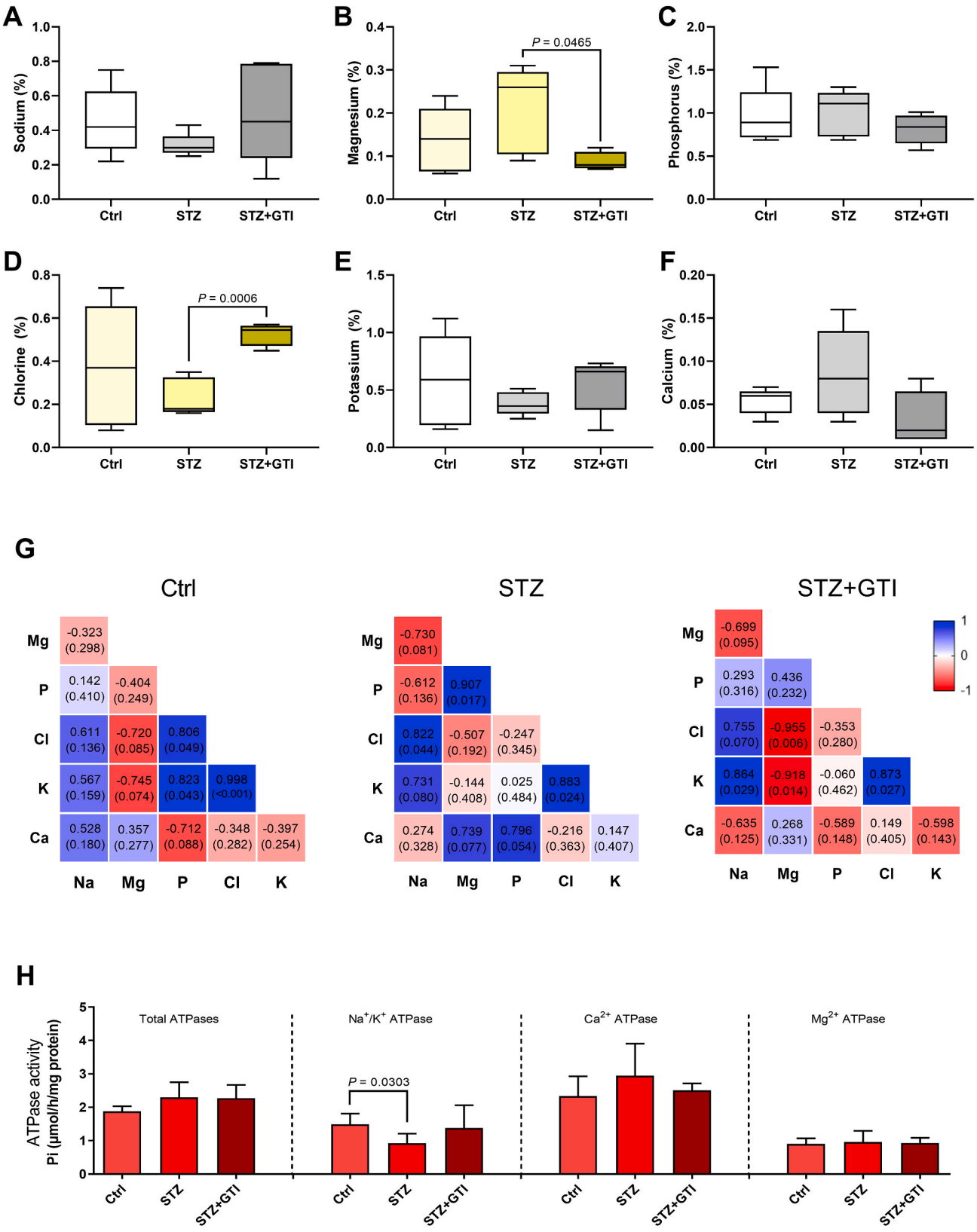

Fig. 4. Microelement proportions and its correlations, and ATPase activity in the kidney of male Wistar diabetic rats treated or not with green tea infusion and a healthy control group. **A** – Sodium (%). **B** – Magnesium (%). **C** – Phosphorus (%). **D** – Chlorine (%). **E** – Potassium (%). **F** – Calcium (%). **G** – Elemental correlations. **H**–Na^+/K^+, Ca^{2+}, Mg^{2+} and total ATPase activity. Mean ± SD. The box represents the interquartile interval with the mean indicated (horizontal line), and the whiskers represent the superior and inferior quartiles. The statistical differences are indicated with lines with the *P*-value above or below them. Data were compared by Student *t*-test (Ctrl vs STZ; STZ vs STZ + GTI) considering statistical differences when $P \leq 0.05$. The correlations were calculated by Pearson's method and the r^2 is shown in the upper number of each graph cell, the bottom number in each graph cell corresponds to the *P*-value of each correlation. (n = 6 animals/group).

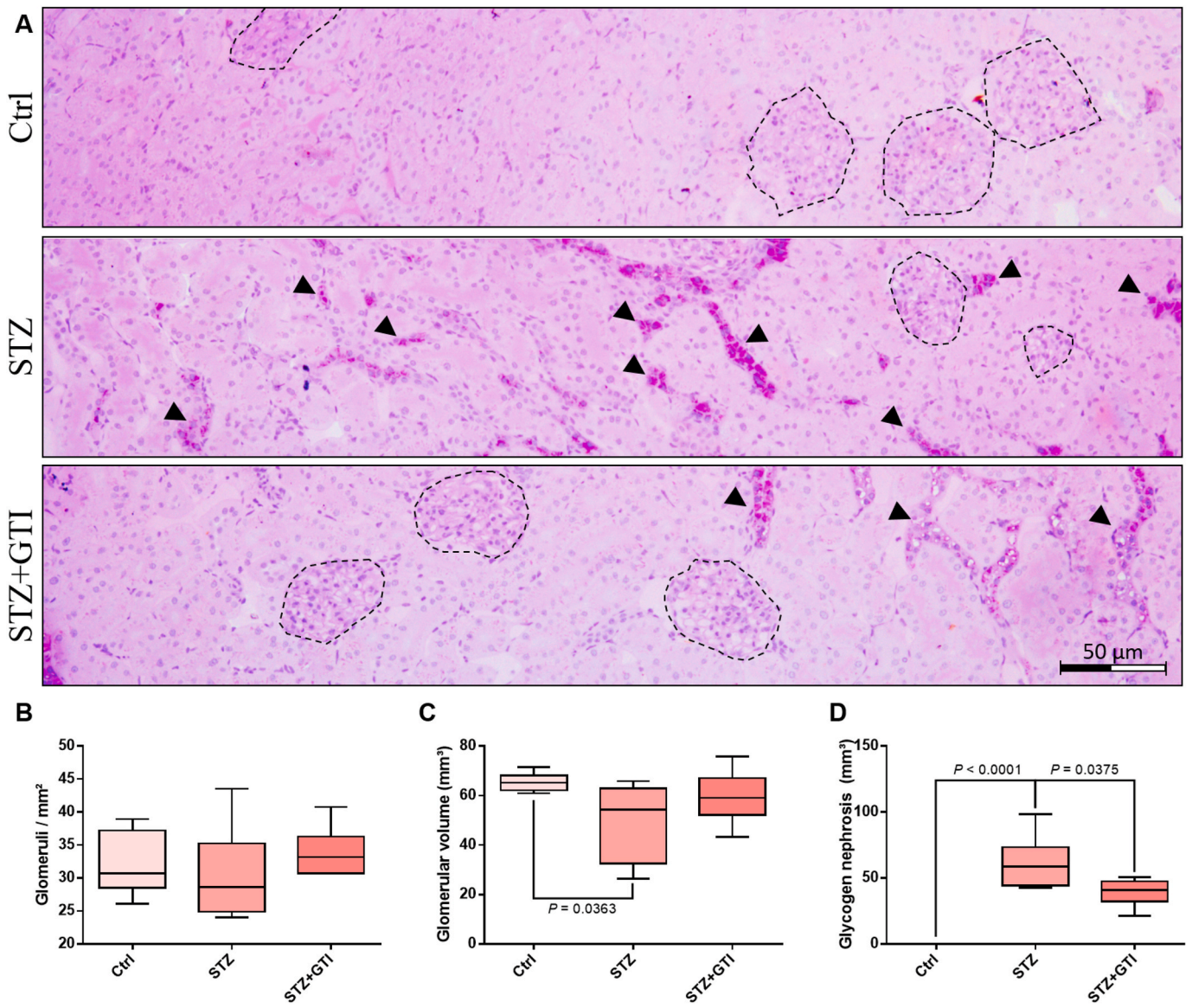

Fig. 5. Representative PAS stained photomicrographs, histopathological and stereological parameters of the kidney's cortex of male Wistar diabetic rats treated or not with green tea infusion and a healthy control group. **A** – Kidney's cortex photomicrography. The glomeruli are delimited by the dotted line. The glycogen nephrosis areas are indicated by the arrowheads. The scale bar is indicated in figure. **B** – Glomeruli/mm^2. **C** – Total glomerular volume (mm^3). **D** – Glycogen nephrosis volume (mm^3). The box represents the interquartile interval with the median indicated (horizontal line), and the whiskers represent the superior and inferior quartiles. The statistical differences are indicated with lines with the *P*-value above or below them. Data were compared by Student *t*-test (Ctrl vs STZ; STZ vs STZ + GTI) considering statistical differences when $P \leq 0.05$. (n = 6 animals/group).

remain between the Ctrl normal reported values, the relationship between all these elements was impaired by diabetes (Fig. 4, G), and GTI was not able to restore the homeostatic environment of ion dynamics. Additionally, we detected a reduced activity of the Na^+/K^+ ATPase pump in the diabetic group (Fig. 4, H). Similarly to the total ATPase activity, the Ca^{2+} and Mg^{2+} ATPases were not affected either.

Histopathological analysis revealed a reduced glomerular volume in the diabetic groups (Fig. 5, C), but no differences in the glomeruli number per area (mm^2) (Fig. 5, B). Sections of the healthy control group did not present any pathological feature, and the measurements are compatible with those described ones for the species. However, the diabetic groups presented an abnormal accumulation of glycogen in the tubules, known as glycogen nephrosis. The volume of glycogen accumulation in the diabetic group increased, compared with the Ctrl group (Fig. 5, D). However, the GTI treatment was able to prevent the glycogen granules accumulation in the diabetic animals (Fig. 5, D).

Diabetes led to a reduced proportion of AO-positive cells in the renal cortex (Fig. 6, A), which indicates a reduced proportion of cells without DNA damage. Consequently, it was observed a increased proportion of IP-positive cells, as shown in Fig. 6, B. On the other hand, GTI was able to counteract these effects by improving the proportion of AO-positive cells (Fig. 6, A), and reducing the proportion of the IP-positive cells (Fig. 6, B).

Glomerular morphological analysis reveals diabetic glomerulus surrounded by flattened epithelial cells with pathological alterations that were less frequent in the group treated with GTI. Diffuse mesangial expansion was more frequently observed in almost every glomeruli in the STZ group. Bowman's capsule lesions were more frequently found in the untreated diabetic than in the STZ + GTI group. Nodular mesangial expansion was not observed in any group. Moderate dilation in the lumen of the proximal tubule was more frequent in the STZ group. Also in the STZ group, the basal region of the proximal tubular cells presented the accumulation of aggregated stained granules, more densely than in the healthy group, possible mitochondria aggregation (Itagaki et al.,

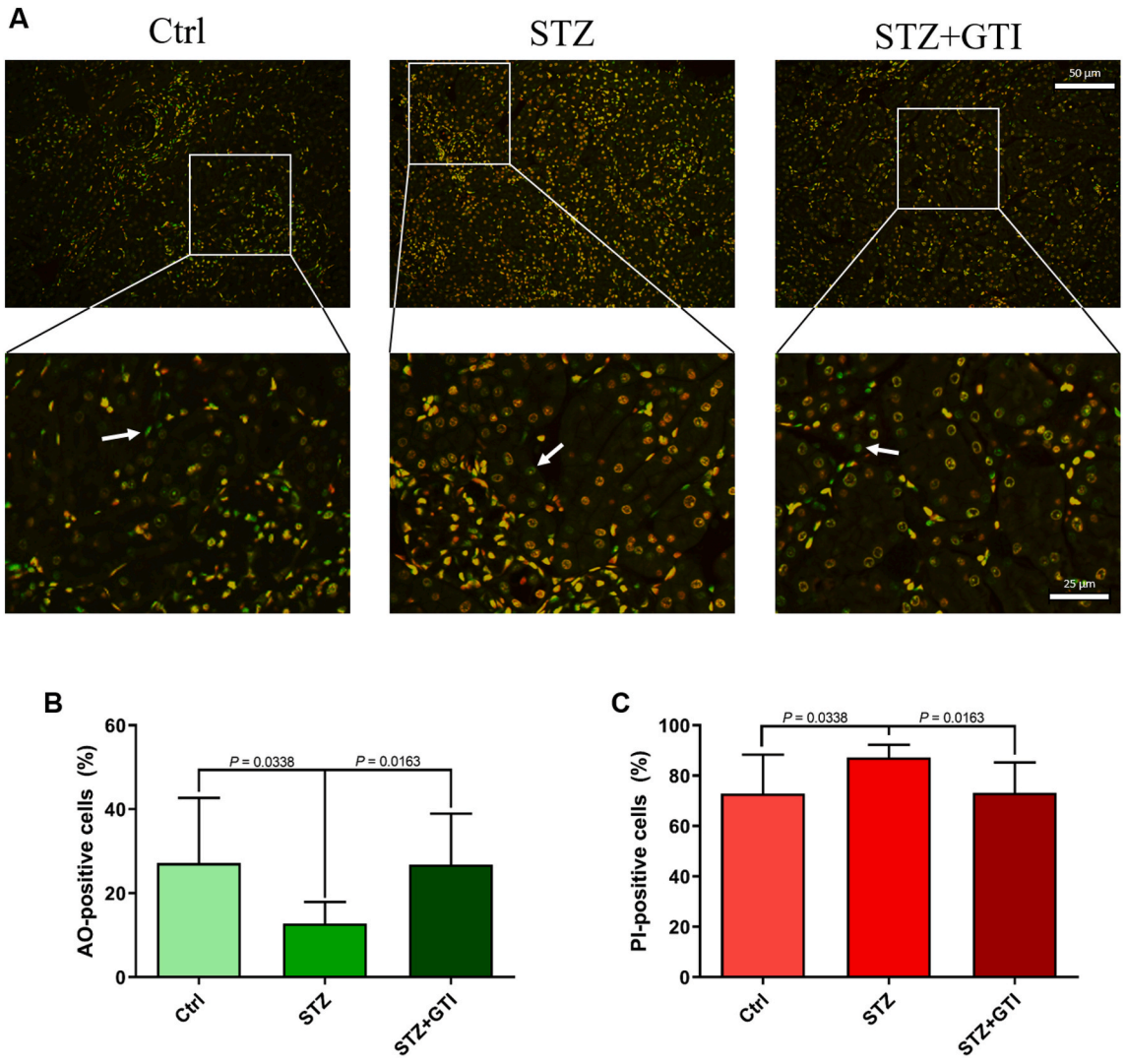

Fig. 6. Representative acridine orange (AO) and propidium iodide (IP) stained photomicrographs of the kidney's cortex of male Wistar diabetic rats treated or not with green tea infusion and a healthy control group. **A** – Kidney's cortex photomicrography. Green nuclei – AO-positive; Yellow to reddish nuclei – IP-positive; Arrows indicate PI-positive nuclei. Scales bars are indicated in figure. **B** – AO-positive cells (%). **C** – IP-positive cells (%). Mean ± SD. The statistical differences are indicated with lines with the *P*-value above them. Data were compared by Student *t*-test (Ctrl vs STZ; STZ vs STZ + GTI) considering statistical differences when $P \leq 0.05$. (n = 6 animals/group).

1995). Furthermore, karyocytomegaly was frequently observed in the STZ group and less frequency in the STZ + GTI group, as so as cytoplasmatic microvesicles, possibly lipid droplets, in the proximal tubule cells (Fig. 7).

3.2. Virtual analysis

The STRING network is presented in Fig. 8, A, and highlights the two main functional clusters (Cluster 1 and Cluster 2). The Reactome Pathway analysis for each cluster is summarized in Table 2. The centrality analysis demonstrated that protein kinase B 1 (AKT1) is the protein classified as the "bottleneck" in the network, with the capacity to integrate the functional pathways that participate in the catechin effects in the kidney (Fig. 8, B). The implications of AKT1 in green tea induced signaling in diabetic nephropathy are discussed below. All proteins in the PPI network are expressed in the normal kidney in different degrees.

4. Discussion

Our results showed that green tea infusion treatment was able to prevent glycogen accumulation in the renal tubules, reduce the DNA damage caused by the hyperglycemic state in renal cortex cells and prevent the aggravation of glomerular morphological alterations, regardless of any hyperglycemia reduction. These outcomes confirm that green tea positive effects on diabetic nephrosis are broader than glycemic regulation related effects. Although our study has not shown a strong improvement in organ function, DNA preservation is determinant in cell survival and proper function, and glomerular morphological integrity is elemental to the filtration process. Such results, together with the *in silico* considerations, may indicate key points in the signaling pathways to improve diabetic nephropathy treatment, as coadjuvant, and prevention, with a herbal medicine, widely distributed and highly accepted around the world.

In adult animals, the kidney weight is increased by the damage caused by hyperglycemia. Such injuries lead to hypertrophy and compensatory hyperplasia in the tubules, in order to preserve the glomerular filtration function, thus increasing the kidney's weight (Herman-Edelstein and Doi, 2016). However, our animals were induced to diabetes at a younger age, so that they had not passed the full development process of the body and organs, including the kidneys, that would still go through a period of growth and subsequent weight gain (Arataki, 1926). The damage caused by hyperglycemia at this stage of

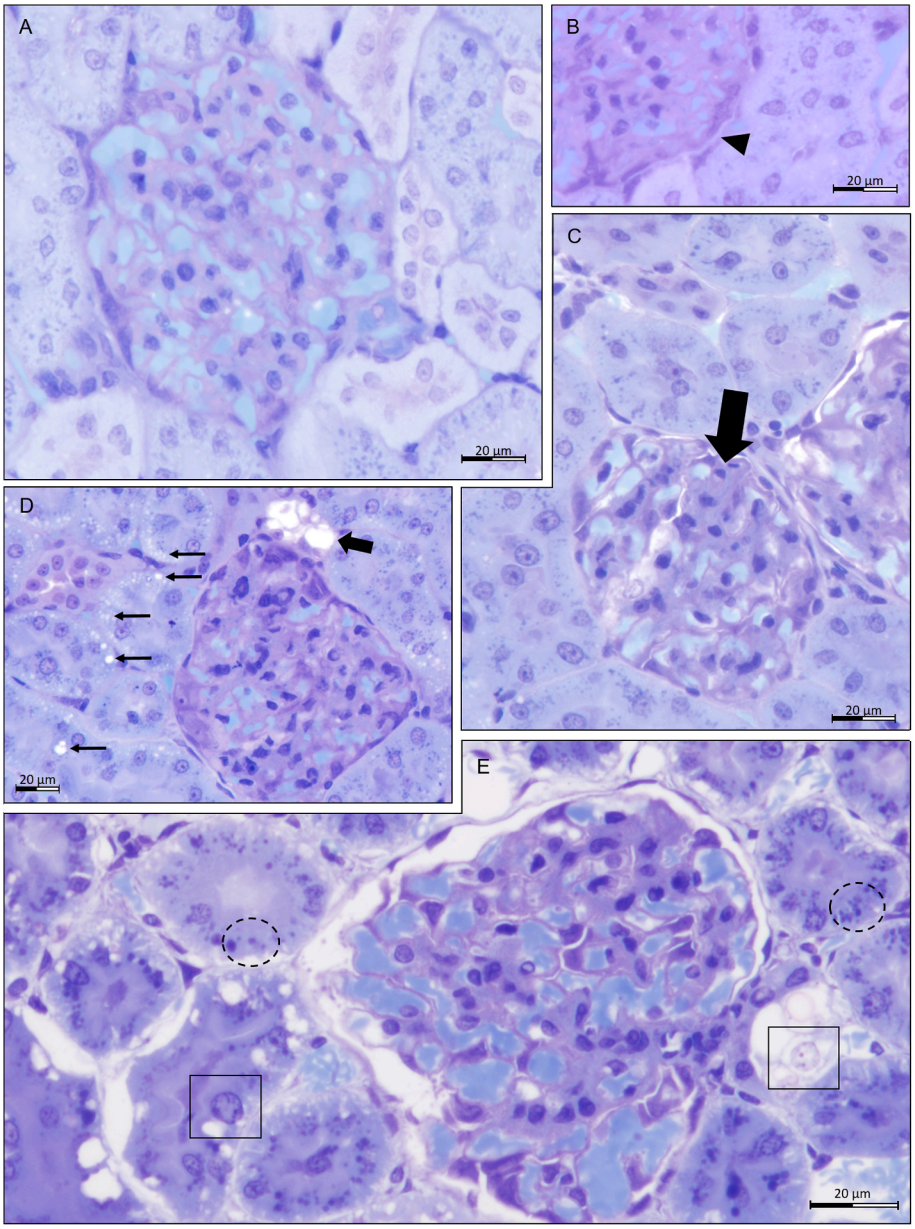

Fig. 7. Representative photomicrographs of the glomerulus, stained with Toluidine Blue – Sodium borate 1%, of male Wistar diabetic rats treated or not with green tea infusion and a healthy control group. **A** – A normal glomeruli of an animal from the healthy control group. **B** – Diabetic glomeruli. Arrowhead indicates a thickening in the glomeruli basal membrane. **C** – Diabetic glomeruli. Arrow indicates a region of diffuse mesangial expansion. **D** – Diabetic glomeruli. Thick arrow indicates a remarkable vacuolization in the macula densa region. Thin arrows indicate cytoplasmic microvesicles in the proximal tubule cells. **E** – Diabetic glomeruli. Squares indicate karyocytomegaly in the proximal tubule. Dotted circles indicate basal regions in the tubular cells with accumulation of stained granules, possible mitochondria aggregation. The glomeruli present a dilated Bowman's space.

life seems to have been severe enough to delay the progression of the organ's normal growth, stagnating the weight gain, as well as the entire development of the animal body, as described in other experimental conditions with young animals (da Silva et al., 2016; Haraguchi et al., 2020; Silva et al., 2009). Besides, such damage may have extended to prevent the green tea's positive effects on kidney function markers found in other studies with adult animals (Hayashi et al., 2020; Renno et al., 2008). Our data suggest that diabetes, when diabetes occurs early, it impairs the development of the kidney, as well as the glomerulus, which is reflected in the low volume of the glomerulus and appearance of pathological features (e.g. mesangial expansion, karyocytomegaly and glomerular basal membrane alterations) in the diabetic animals, compared to the healthy control. Although we have not observed statistical difference, the size of the glomerulus presented a higher mean and lower variance (SD) in the group treated with green tea, compared with the diabetic one, thus approaching the characteristics that describe the control group. Such data are in line with the protective effects on glomerular morphology exercised by EGCG, the main catechin found in green tea (Yoon et al., 2014).

It is known that catechins in green tea have a hypoglycemic and preventive effect on high glucose levels (Fu et al., 2017), and it was assumed that the beneficial effects of green tea in diabetic nephropathy, especially concerning the tubular glycogen nephrosis, were due to this hypoglycemiant capacity (Renno et al., 2008). However, green tea treatment, or its isolated catechin administration, can generate positive outcomes without the achievement of proper glycemic control (Hayashi et al., 2020), confirming that the tea's effect on diabetes goes beyond improving glucose-related harms.

Glycogen accumulation in renal tubules, as presented in our study, is a hallmark of experimental diabetic nephropathy induced by STZ or Alloxan in experimental models (Kang et al., 2005). Under normal conditions, glucose is reabsorbed almost completely in the proximal tubule by sodium-dependent glucose transporter 2 (SGLT2) and, in lower levels, by sodium-dependent glucose transporter 1 (SGLT1), and appears in the urine when the absorptive capacity is extrapolated (Bailey, 2011; Vallon and Thomson, 2017). Additionally, proximal tubule cells have greater capacity to perform gluconeogenesis from lactate, glutamine and glycerol,wich is an upregulated process in

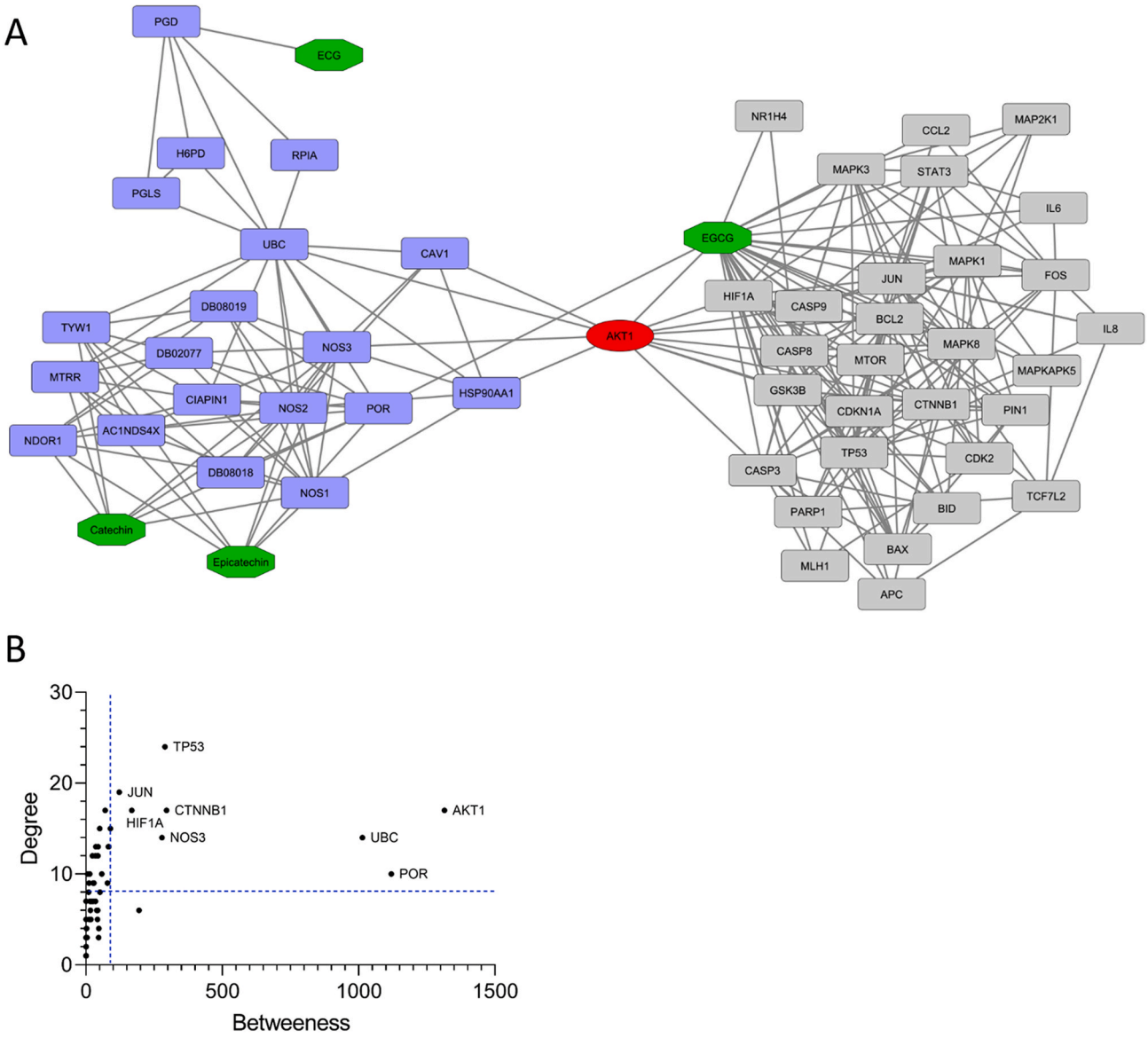

Fig. 8. *In silico* exploration of catechins effects in the kidney. **A** – Compound-Protein Interactome network, highlighting tea catechins (green nodes), bottleneck protein (red node), cluster 1 (grey nodes), and cluster 2 (light blue nodes). **B** – Centrality analysis for the CPI network, the blue lines represent the threshold of the parameter.

diabetes (Eid et al., 2006). The glycogen accumulated in the tubule may result from the sum of factors including abnormally increased absorption, and increased gluconeogenesis (Herman-Edelstein and Doi, 2016; Mather and Pollock, 2011).

Green tea catechins are shown to act as SGLT1 inhibitors *in vitro* (Kobayashi et al., 2000), wihch suggests that tea treatment forces the glucose reabsorption process in the kidney to be carried out by SGLT2 alone. At the time, there is no evidence suggesting an inhibitory effect of catechins on SGLT2. However, EGCG was shown to inhibit glucose production via gluconeogenesis in cells by activating AMPK (Collins et al., 2007). Besides, EGCG suppresses gluconeogenic gene expression (e.g. glucose-6-phosphatase and phosphoenolpyruvate carboxykinase) via the phosphoinositide 3-kinase (PI3K) pathway (Waltner-Law et al., 2002). Such a mechanism in kidney cells could reduce glucose overload and the improvement of glycogen accumulation in proximal tubules and may explain the positive outcomes of GTI treatment in our study.

Furthermore, diabetes can increase the expression of SGLT2 and sodium-hydrogen antiporter 3 (NHE3), in response to the higher demand for adenosine triphosphate (ATP) to maintain the glucose reabsorption flow (Herman-Edelstein and Doi, 2016). The great capacity of tubular cells to perform gluconeogenesis, a process that consumes a lot of ATP, further increases the demand for the molecule (Gilbert, 2017). Such increased demand for energy therefore enhances the oxygen (O_2) demand creating a hypoxic environment in the tubular cells (Herman-Edelstein and Doi, 2016). However, the blood supply of O_2 in this case is severely affected by the endothelial damage caused by glucose, which leads to loss and obstruction of capillaries, worsen the oxygen supply (Herman-Edelstein and Doi, 2016). In this way, a deeper hypoxic environment is generated, favorable to the activation of apoptosis via the Caspase pathway, and the fibrosis development in the organ by stimulating the Transforming growth factor-beta (TGF-β) pathway. In turn, the progression of fibrosis further worsens hypoxia, aggravating cell death in the organ (Gilbert, 2017). This mechanism is also accompanied by increased expression of stem cell factor (SCF) and proto-oncogene c-kit (c-kit) (Yin et al., 2018). In contrast, ellagic acid, a derivative polyphenol found in green tea (Yang and Tomás-Barberán, 2019), is shown to inhibit tyrosinase activity (Yoshimura et al., 2005), inhibiting the SCT-Kit pathway and alleviating the damages caused by

Table 2
Reactome pathways identified for each cluster with specific interest to the diabetic nephropathy pathological state, identified by the comparison of the CPI network with the Reactome Pathway database with the corresponding adjusted P-values.

Cluster	Proteins	Reactome Pathway	Adjusted *P*-value
Cluster 1	NR1H4, CCL2, IL8, IL6, MAPKAPK5, STAT3, PIN1, PARP1, CASP8, MTOR, MAPK3, MAPK8, MLH1, CASP3, CASP9, GSK3B, HIF1A, BID, MAPK1, MAP2K1, BAX, BCL2, FOS, JUN, APC, AKT1, CDKN1A, CDK2, TP53, CTNNB1, TCF7L2	Apoptosis	1.76×10^{-7}
		Signaling by SCF-KIT	1.06×10^{-6}
		Signaling by FGFR in disease	4.35×10^{-6}
		Signaling by PDGF	6.00×10^{-6}
		TRIF-mediated TLR3/TLR4 signaling	6.00×10^{-6}
		AKT phosphorylates targets in the cytosol	1.15×10^{-5}
Cluster 2	DB02077, RPIA, POR, H6PD, PGLS, PGD, AKT1, TYW1, MTRR, NOS2, DB08019, DB08018, AC1NDS4X, NOS1, CAV1, NDOR1, CIAPIN1, HSP90AA1, UBC, NOS3	eNOS activation	1.05×10^{-6}
		Pentose phosphate pathway	1.30×10^{-5}
		AKT phosphorylates targets in the cytosol	3.70×10^{-5}
		Metabolism of carbohydrates	1.53×10^{-4}
		Cellular response to hypoxia	1.50×10^{-3}
		PI3K/AKT/mTOR activation	6.29×10^{-3}

hypoxia.

Accordingly, green tea extract can inhibit the fibroblast growth factor receptor (FGFR) signaling by reducing the expression of fibroblast growth factor (FGF) (Sartippour et al., 2002). In addition, EGCG impedes the signaling pathway of the platelet-derived growth factor (PDGF), other profibrotic factors (Park et al., 2006).

Hypoxia can aggravate diabetic kidney disease by upregulating the expression of Toll-Like Receptor 4 (TLR4) ligands in diabetes, as fibronectin (Zhang et al., 2018) and high-mobility group box 1 (HMGB1) (Feng et al., 2020). The activation of the TLR4 signal mediated by the TIR-domain-containing adaptor-inducing Interferon-β (TRIF) culminates in the activation of the nuclear factor κ B (NfκB), wich lead to inflammation and fibrosis in the kidney (Feng et al., 2020). However, EGCG proved to inhibit the TLR pathway activation *in vitro* (Youn et al., 2006) and to reduce the NfκB expression (Yamabe et al., 2006), wich suggests that tea may act through this mechanism to promote anti-inflammatory and antifibrotic protection in the kidney.

Our results demonstrated that green tea was able to reduce the binding of propidium iodide to DNA and enhance GST activity, suggesting an improvement in DNA integrity or that there was some reduction in the damage caused by hyperglycemia or oxidizing agents. A previous study reported that EGCG can inhibit apoptosis induced by oxidative stress (Itoh et al., 2005) and preserve renal cells in an *in vitro* model. Also, green tea polyphenols can contribute to reduce apoptosis levels in diabetic nephropathy by blocking the glycogen synthase kinase-3 β (GSK3β) interaction with the tumor protein 53 (TP53), wich reduces Caspase 3 activity in podocytes and increases cell survival rates (Borges et al., 2016; Peixoto et al., 2015). A review study by Mohabbulla Mohib et al. (2016) summarizes other possible mechanisms that green tea protects the nuclear envelope and the genome, including the stabilization of the DNA strand and also the reduction of NF-κB expression culminating in the already discussed positive outcomes.

The homeostatic maintenance of the ions inside the cell may affect the antioxidant enzyme activities (Soetan et al., 2010). Our results demonstrate that green tea was not able to reverse the dysregulation in the relationship between the ions in the kidneys, which actively participate in the functioning of antioxidant enzymes. Also, oxidative stress may be responsible to inhibit Na^+/K^+ ATPase activity by the oxidation of thiol groups in the pumps (Al-Numair et al., 2015). Despite the increased GST activity shown in our study, the Na^+/K^+ ATPase function was not recovered.

The PI3K/AKT/mammalian target of the rapamycin (mTOR) pathway is linked to metabolic regulation in diabetic nephropathy and the development of human kidney cancer. This signal cascade is upregulated in diabetes and is closely related to glycogen tubular accumulation (Ribback et al., 2015). EGCG proved to inhibit both PI3K and mTOR, by competitively binding in the ATP-binding sites in these proteins (Van Aller et al., 2011). Additionally, mTOR inhibition can restore the autophagy mechanism, reduced by mTOR overexpression in diabetes, and contribute to cellular renovation in the kidney. Also, the PI3K/AKT/mTOR pathway is related to *de novo* lipogenesis in the kidney (Ribback et al., 2015), which can lead to lipid accumulation, as in line with the microvesicles showed in Fig. 6 D. Green tea treated animals did not present this cytoplasmic microvesicles.

Our *in silico* results demonstrate that protein kinase B (AKT) is the central protein in the catechin mediated effects in the kidney. EGCG can activate the diacylglycerol kinase (DGK) pathway, thus promoting the inactivation of protein kinase C beta (PKC-β) and improving the condition of diabetic nephropathy (Hayashi et al., 2020). Such a process is initiated by the interaction of EGCG with the 67-kDa laminin receptor (67LR), which is known as an EGCG receptor (Tachibana et al., 2004) and is also capable of activating the AKT in the kidney (Kumazoe et al., 2020). Hayashi et al. (2015) showed that EGCG activates DGK-α via 67LR binding. In a recent study (Hayashi et al., 2020), the authors proposed that this mechanism occurs by activating 67LR receptors in the cell membrane, which, when activated, promotes the translocation of the DGK to the membrane, through the formation of 67LR-DGK-α and α3-β1 integrin's complex. This increases focal adhesion of podocyte foot process in the glomerular basement membrane, thus ensuring cell adhesion, in addition to inhibiting α and β PKC (Hayashi, 2020), preserving glomerular morphology. This mechanism may be responsible for the positive effects on glomerular preservation by green tea ingestion. Other catechins present in green tea composition may exert effect by the AKT pathway activation by a different receptor, as they do not bind with the 67LR (Tachibana et al., 2004). However the primary membrane receptor for them is still unknown.

5. Conclusion

The components of green tea can interact with proteins participating in cell signaling pathways that regulate energy metabolism, including glucose and glycogen synthesis, glucose reabsorption, hypoxia management, and cell death by apoptosis. Such interaction reduces the accumulation of glycogen in the kidney's cells of the proximal tubules in diabetes, as well as DNA damage. These results also reflect in a preserved glomerulus morphology, with improvement in pathological features, and suggests the prevention of kidney function impairment. Our results demonstrate that such benefits are achieved regardless of the blood glucose status, or the hyperglycemia reduction to be achieved.

Declaration of competing interest

The authors have no conflicts of interest to disclose.

Acknowledgments

The authors are grateful to Bioclin Laboratories for kindly providing the biochemical kits used in this work; "Laboratório de Microscopia Eletrônica" of the Physics Department of the Federal University of Viçosa; Eliana Alviarez Gutierrez, for the green tea infusion chemical analysis; Letícia Monteiro Farias, of the "Laboratório de Biodiversidade" of the Biochemistry and Molecular Biology Department of the Federal University of Viçosa, for the chemical analysis of the green tea infusion

in HPLC; Diego Dominik for the assistance with logistics and the experiment; Professor Dr. Marcio Roberto Silva, for the statistical insights; Enedina Sacramento, for the English proofreading service; we also thank the two anonymous reviewers for their valuable comments, and Coordenação de Aperfeiçoamento de Pessoal de Nível Superior (CAPES), for the L. C. M. Ladeira Ph.D. scholarship provided (Procs. Nr. 88882.436984/2019–01).

Abbreviations

67LR 67 kDa laminin receptor
ABTS 2,2′-Azinobis-[3-ethylbenzthiazoline-6-sulfonic acid]
NOS1 Nitric Oxide Synthase 1
AGE/RAGE advanced glycated end-products and its receptor
AKT protein kinase B
AMPK 5′-AMP-activated protein kinase
AO acridine Orange
APC APC Regulator Of WNT Signaling Pathway
ATP adenosine triphosphate
BAX BCL2 Associated X
BCL2 BCL2 Apoptosis Regulator
BID BH3 Interacting Domain Death Agonist
BW body weight
Ca calcium
CaCl calcium chloride;
CASP3 Caspase 3
CASP8 Caspase 8
CASP9 Caspase 9
CAT catalase
CAV1 Caveolin 1
CCL2 C–C Motif Chemokine Ligand 2
CDK2 Cyclin Dependent Kinase 2
CDKN1A Cyclin Dependent Kinase Inhibitor 1
CIAPIN1 Cytokine Induced Apoptosis Inhibitor 1
c-kit proto-oncogene c-kit
Cl chlorine;
CPI compound-protein interactions
CTNNB1 Catenin Beta 1
Ctrl control group;
DB02077 L-N(omega)-nitroarginine-(4 R)-amino-L-proline amide (NOS3)
DB08019, DB08018 and NOS3 Nitric Oxide Synthase 3
DKG diacylglycerol kinase
DN Diabetic nephropathy
EGCG epigallocatechin gallate
FGF fibroblast growth fator
FGFR fibroblast growth factor receptor
FOS Fos Proto-Oncogene
FRAP ferric reducing antioxidant power
GSK3β glycogen synthase kinase-3 β
GST glutathione S-transferase
GTI Green tea infusion
H_2O_2 hydrogen peroxide;
H6PD Hexose-6-Phosphate Dehydrogenase/Glucose 1-Dehydrogenase
HIF1A Hypoxia Inducible Factor 1 Subunit Alpha
HMG1 high-mobility group box 1
HSP90AA1 Heat Shock Protein 90 Alpha Family Class A Member 1
i.p. intraperitoneal
IL6 Interleukin 6
IL8 Interleukin 8
JUN Jun Proto-Oncogene
K potassium
KCl potassium chloride;
KW kidney weight
MAP2K1 Mitogen-Activated Protein Kinase Kinase 1
MAPK1 Mitogen-Activated Protein Kinase 1
MAPK3 Mitogen-Activated Protein Kinase 3
MAPK8 Mitogen-Activated Protein Kinase 8
MAPKAPK5 MAPK Activated Protein Kinase 5
Mg magnesium
MgCl magnesium chloride
MLH1 MutL Homolog 1
mTOR – mammalian target of rapamycin
MTRR 5-Methyltetrahydrofolate-Homocysteine Methyltransferase Reductase
Na sodium
NaCl sodium chloride;
NADPH reduced nicotinamide adenine dinucleotide phosphate
NDOR1 NADPH-dependent diflavin reductase
NfκB nuclear factor κ B
NO_2^-/NO_3^- nitric oxide;
NOS2 Nitric Oxide Synthase 2
NR1H4 Nuclear Receptor Subfamily 1 Group H Member 4
O_2 oxygen
O^-_2 superoxide;
PARP1 Poly(ADP-Ribose) Polymerase 1
PDGF platelet-derived growth fator
PGD Phosphogluconate Dehydrogenase
PGLS 6-Phosphogluconolactonase
PI propidium iodide
PI3K phosphoinositide 3-kinase
PIN1 Peptidylprolyl Cis/Trans Isomerase,NIMA-Interacting 1
PKC-β protein kinase C beta
POR Cytochrome P450 Oxidoreductase
PPI Protein-Protein Interactome
RPIA Ribose 5-Phosphate Isomerase A
RSI renal somatic index
SCF stem cell fator
SD standard deviation
SGLT1 sodium-dependent glucose transporter 1
SGLT2 sodium-dependent glucose transporter 2
SOD superoxide dismutase
SOES Specific Organ Expression Score
STAT3 Signal transducer and activator of transcription 3
STZ streptozotocin
TCA Trichloroacetic acid
TCF7L2 Transcription Factor 7 Like 2
TE Trolox equivalente
TGF-β transforming growth factor-beta
TLR4 toll-like receptor 4
TP53 tumor protein 53
TRIF TIR domain-containing adaptor-inducing Interferon- β;
TYW1 TRNA-YW Synthesizing Protein 1 Homolog
UBC Ubiquitin C

Authors' contributions

LCML planned and carried the experiment, performed the analysis and interpreted the results, wrote the original draft, reviewed and final edited the manuscript. ECS participate in the conceptualization of the experiment, interpretation of results and writing of the manuscript. TAS, JS, GDAL, performed the analysis, interpreted results, reviewed and approved the final manuscript. MMN participate in the conceptualization of the experiment, provided resources, reviewed and approved the final manuscript. RCS and MBF provided resources, participate in the interpretation of results, reviewed and approved the final manuscript. IRSCM participate in the conceptualization of the experiment, interpretation of results, supervision and administration of the project, reviewed and approved the final manuscript.

Availability of data and material

The datasets used and/or analyzed during the current study are available from the corresponding author on reasonable request.

Ethics statement

The use of animals in this study was approved by the Ethics Committee of Animal Use of the Federal University of Viçosa (CEUA/UFV – protocol number 53/2018).

Funding

This paper was supported by a grant from the Brazilian agency CAPES (Coordenação de Aperfeiçoamento de Pessoal de Nível Superior, Procs. Nr. 88882.436984/2019–01) and resources from the CNPq (Conselho Nacional de Desenvolvimento Científico e Tecnológico, Chamada UNIVERSAL, 2018; Procs. Nr. 431,330/2018-2).

References

Aebi, H., 1984. [13] Catalase in vitro. In: Methods in Enzymology, Methods in Enzymology. Elsevier, pp. 121–126. https://doi.org/10.1016/S0076-6879(84)05016-3.

Al-Numair, K.S., Veeramani, C., Alsaif, M.A., Chandramohan, G., 2015. Influence of kaempferol, a flavonoid compound, on membrane-bound ATPases in streptozotocin-induced diabetic rats. Pharm. Biol. 53, 1372–1378. https://doi.org/10.3109/13880209.2014.982301.

Arataki, M., 1926. On the postnatal growth of the kidney, with special reference to the number and size of the glomeruli (albino rat). Am. J. Anat. 36, 399–436. https://doi.org/10.1002/aja.1000360302.

Bader, G.D., Hogue, C.W.V., 2003. An automated method for finding molecular complexes in large protein interaction networks. BMC Bioinf. 4, 1–27. https://doi.org/10.1186/1471-2105-4-2.

Bailey, C.J., 2011. Renal glucose reabsorption inhibitors to treat diabetes. Trends Pharmacol. Sci. 32, 63–71. https://doi.org/10.1016/j.tips.2010.11.011.

Barkaoui, M., Katiri, A., Boubaker, H., Msanda, F., 2017. Ethnobotanical survey of medicinal plants used in the traditional treatment of diabetes in Chtouka Ait Baha and Tiznit (Western Anti-Atlas), Morocco. J. Ethnopharmacol. 198, 338–350. https://doi.org/10.1016/j.jep.2017.01.023.

Bernas, T., Asem, E.K., Robinson, J.P., Cook, P.R., Dobrucki, J.W., 2005. Confocal fluorescence imaging of photosensitised DNA denaturation in cell nuclei. Photochem. Photobiol. 33342, 960–969. https://doi.org/10.1562/2004-11-11-ra-369.

Bindea, G., Galon, J., Mlecnik, B., 2013. CluePedia Cytoscape plugin: pathway insights using integrated experimental and in silico data. Bioinformatics 29, 661–663. https://doi.org/10.1093/bioinformatics/btt019.

Bindea, G., Mlecnik, B., Hackl, H., Charoentong, P., Tosolini, M., Kirilovsky, A., Fridman, W.H., Pagès, F., Trajanoski, Z., Galon, J., 2009. ClueGO: a Cytoscape plug-in to decipher functionally grouped gene ontology and pathway annotation networks. Bioinformatics 25, 1091–1093. https://doi.org/10.1093/bioinformatics/btp101.

Borges, C.M., Papadimitriou, A., Duarte, D.A., Lopes De Faria, J.M., Lopes De Faria, J.B., 2016. The use of green tea polyphenols for treating residual albuminuria in diabetic nephropathy: a double-blind randomised clinical trial. Sci. Rep. 6, 1–9. https://doi.org/10.1038/srep28282.

Chopade, V.V., Phatak, A.A., Upaganlawar, A.B., Tankar, A.A., 2008. Green tea (Camellia sinensis): chemistry , traditional , medicinal uses and its pharmacological activities-a review. Phcog. Rev. 2, 157–162.

Collins, Q.F., Liu, H.-Y.Y., Pi, J., Liu, Z., Quon, M.J., Cao, W., 2007. Epigallocatechin-3-gallate (EGCG), A green tea polyphenol, suppresses hepatic gluconeogenesis through 5′-AMP-activated protein kinase. J. Biol. Chem. 282, 30143–30149. https://doi.org/10.1074/jbc.M702390200.

da Silva, E., Natali, A.J., da Silva, M.F., de Jesus Gomes, G., da Cunha, D.N.Q., Toledo, M. M., Drummond, F.R., Ramos, R.M.S., dos Santos, E.C., Novaes, R.D., de Oliveira, L.L., Maldonado, I.R., dos, S.C., 2016. Swimming training attenuates the morphological reorganization of the myocardium and local inflammation in the left ventricle of growing rats with untreated experimental diabetes. Pathol. Res. Pract. 212, 325–334. https://doi.org/10.1016/j.prp.2016.02.005.

de Godoi, R.S., Almerão, M.P., da Silva, F.R., 2020. In silico evaluation of the antidiabetic activity of natural compounds from Hovenia dulcis Thunberg. J. Herb. Med. 100349. https://doi.org/10.1016/j.hermed.2020.100349.

Dias, F.C.R., Martins, A.L.P., de Melo, F.C.S.A., Cupertino, M. do C., Gomes, M. de L.M., de Oliveira, J.M., Damasceno, E.M., Silva, J., Otoni, W.C., da Matta, S.L.P., 2019. Hydroalcoholic extract of Pfaffia glomerata alters the organization of the seminiferous tubules by modulating the oxidative state and the microstructural reorganization of the mice testes. J. Ethnopharmacol. 233, 179–189. https://doi.org/10.1016/j.jep.2018.12.047.

Dieterich, S., Bieligk, U., Beulich, K., Hasenfuss, G., Prestle, J., 2000. Gene expression of antioxidative enzymes in the human Heart : increased expression of catalase in the end-stage failing heart. Circulation 101, 33–39. https://doi.org/10.1161/01.CIR.101.1.33.

Eid, A., Bodin, S., Ferrier, B., Delage, H., Boghossian, M., Martin, M., Baverel, G., Conjard, A., 2006. Intrinsic gluconeogenesis is enhanced in renal proximal tubules of Zucker diabetic fatty rats. J. Am. Soc. Nephrol. 17, 398–405. https://doi.org/10.1681/ASN.2005070742.

Fallah Huseini, H., Fakhrzadeh, H., Larijani, B., Shikh Samani, A.H., 2006. Review of anti-diabetic medicinal plant used in traditional medicine. J. Med. Plants 5, 1–8.

Feng, Q., Liu, D., Lu, Y., Liu, Z., 2020. The interplay of renin-angiotensin system and toll-like receptor 4 in the inflammation of diabetic nephropathy. J. Immunol. Res. 2020, 1–11. https://doi.org/10.1155/2020/6193407.

Fiske, C.C.H., Subbarow, Y.Y., 1925. The colorimetric determination of phosphorus. J. Biol. Chem. 66, 375–400.

Fu, Q.-Y., Li, Q.-S., Lin, X.-M., Qiao, R.-Y., Yang, R., Li, X.-M., Dong, Z.-B., Xiang, L.-P., Zheng, X.-Q., Lu, J.-L., Yuan, C.-B., Ye, J.-H., Liang, Y.-R., 2017. Antidiabetic effects of tea. Molecules 22, 849. https://doi.org/10.3390/molecules22050849.

Gilbert, R.E., 2017. Proximal tubulopathy: prime mover and key therapeutic target in diabetic kidney disease. Diabetes 66, 791–800. https://doi.org/10.2337/db16-0796.

Habig, W.H., Pabst, M.J., Jakoby, W.B., 1974. Glutathione S-Transferases: the first enzymatic step in mercapturic acid formation. J. Biol. Chem. 25, 7130–7139.

Haraguchi, R., Kohara, Y., Matsubayashi, K., Kitazawa, R., Kitazawa, S., 2020. New insights into the pathogenesis of diabetic nephropathy: proximal renal tubules are primary target of oxidative stress in diabetic kidney. Acta Histochem. Cytoc. 53, 21–31. https://doi.org/10.1267/ahc.20008.

Hayashi, D., Ueda, S., Yamanoue, M., Saito, N., Ashida, H., Shirai, Y., 2015. Epigallocatechin-3-gallate activates diacylglycerol kinase alpha via a 67 kDa laminin receptor: a possibility of galloylated catechins as functional food to prevent and/or improve diabetic renal dysfunctions. J. Funct. Foods 15, 561–569. https://doi.org/10.1016/j.jff.2015.04.005.

Hayashi, D., Wang, L., Ueda, S., Yamanoue, M., Ashida, H., Shirai, Y., 2020. The mechanisms of ameliorating effect of a green tea polyphenol on diabetic nephropathy based on diacylglycerol kinase α. Sci. Rep. 10, 1–12. https://doi.org/10.1038/s41598-020-68716-6.

Herman-Edelstein, M., Doi, S.Q., 2016. Pathophysiology of Diabetic Nephropathy, Proteinuria: Basic Mechanisms, Pathophysiology and Clinical Relevance. Elsevier Inc. https://doi.org/10.1007/978-3-319-43359-2_4.

Itagaki, S. ichi, Nishida, E., Lee, M.J., Doi, K., 1995. Histopathology of subacute renal lesions in mice induced by streptozotocin. Exp. Toxicol. Pathol. 47, 485–491. https://doi.org/10.1016/S0940-2993(11)80332-5.

Itoh, Y., Yasui, T., Okada, A., Tozawa, K., Hayashi, Y., Kohri, K., 2005. Examination of the anti-oxidative effect in renal tubular cells and apoptosis by oxidative stress. Urol. Res. 33, 261–266. https://doi.org/10.1007/s00240-005-0465-7.

Jassal, B., Matthews, L., Viteri, G., Gong, C., Lorente, P., Fabregat, A., Sidiropoulos, K., Cook, J., Gillespie, M., Haw, R., Loney, F., May, B., Milacic, M., Rothfels, K., Sevilla, C., Shamovsky, V., Shorser, S., Varusai, T., Weiser, J., Wu, G., Stein, L., Hermjakob, H., D'Eustachio, P., 2020. The reactome pathway knowledgebase. Nucleic Acids Res. 48, D498–D503. https://doi.org/10.1093/nar/gkz1031.

Kang, J., Dai, X.-S., Yu, T.-B., Wen, B., Yang, Z.-W., 2005. Glycogen accumulation in renal tubules, a key morphological change in the diabetic rat kidney. Acta Diabetol. 42, 110–116. https://doi.org/10.1007/s00592-005-0188-9.

Kim-Park, W.K., Allam, E.S., Palasuk, J., Kowolik, M., Park, K.K., Windsor, L.J., 2016. Green tea catechin inhibits the activity and neutrophil release of Matrix Metalloproteinase-9. J. Tradit. Complement. Med. 6, 343–346. https://doi.org/10.1016/j.jtcme.2015.02.002.

Kobayashi, Y., Suzuki, M., Satsu, H., Arai, S., Hara, Y., Suzuki, K., Miyamoto, Y., Shimizu, M., 2000. Green tea polyphenols inhibit the sodium-dependent glucose transporter of intestinal epithelial cells by a competitive mechanism. J. Agric. Food Chem. 48, 5618–5623. https://doi.org/10.1021/jf0006832.

Kumazoe, M., Fujimura, Y., Tachibana, H., 2020. 67-kDa laminin receptor mediates the beneficial effects of green tea polyphenol EGCG. Curr. Pharmacol. Rep. https://doi.org/10.1007/s40495-020-00228-3.

Ladeira, L.C.M., dos Santos, E.C., Mendes, B.F., Gutierrez, E.A., Santos, C.F.F., de Souza, F.B., Machado-Neves, M., Maldonado, I.R., dos, S.C., 2020a. Green tea infusion aggravates nutritional status of the juvenile untreated STZ-induced type 1 diabetic rat. bioRxiv 35. https://doi.org/10.1101/2020.01.13.904896.

Ladeira, L.C.M., dos Santos, E.C., Valente, G.E., da Silva, J., Santos, T.A., dos Santos Costa Maldonado, I.R., 2020b. Could biological tissue preservation methods change chemical elements proportion measured by energy dispersive X-ray spectroscopy? Biol. Trace Elem. Res. 196, 168–172. https://doi.org/10.1007/s12011-019-01909-x.

Lima, G.D. de A., Sertorio, M.N., Souza, A.C.F., Menezes, T.P., Mouro, V.G.S., Gonçalves, N.M., Oliveira, J.M. de, Henry, M., Machado-Neves, M., 2018. Fertility in male rats: disentangling adverse effects of arsenic compounds. Reprod. Toxicol. 78, 130–140. https://doi.org/10.1016/j.reprotox.2018.04.015.

Lowry, O.H., Rosebrough, N.J., Farr, A.L., Randal, R.J., 1994. Protein measurement with the Folin phenol reagent. Anal. Biochem. 217, 220–230. https://doi.org/10.1016/0304-3894(92)87011-4.

Mather, A., Pollock, C., 2011. Glucose handling by the kidney. Kidney Int. 79, S1–S6. https://doi.org/10.1038/ki.2010.509.

Meng, J.-M., Cao, S.-Y., Wei, X.-L., Gan, R.-Y., Wang, Y.-F., Cai, S.-X., Xu, X.-Y., Zhang, P.-Z., Li, H.-B., 2019. Effects and mechanisms of tea for the prevention and management of diabetes mellitus and diabetic complications: an updated review. Antioxidants 8, 170. https://doi.org/10.3390/antiox8060170.

Mineharu, Y., Koizumi, A., Wada, Y., Iso, H., Watanabe, Y., Date, C., Yamamoto, A., Kikuchi, S., Inaba, Y., Toyoshima, H., Kondo, T., Tamakoshi, A., 2011. Coffee, green tea, black tea and oolong tea consumption and risk of mortality from cardiovascular

disease in Japanese men and women. J. Epidemiol. Community Health 65, 230–240. https://doi.org/10.1136/jech.2009.097311.
Mohabbulla Mohib, M., Fazla Rabby, S.M., Paran, T.Z., Mehedee Hasan, M., Ahmed, I., Hasan, N., Abu Taher Sagor, M., Mohiuddin, S., 2016. Protective role of green tea on diabetic nephropathy - a review. Cogent Biol. 2 https://doi.org/10.1080/23312025.2016.1248166.
Park, J.S., Kim, M.H., Chang, H.J., Kim, K.M., Kim, S.M., Shin, B.A., Ahn, B.W., Jung, Y. D., 2006. Epigallocatechin-3-gallate inhibits the PDGF-induced VEGF expression in human vascular smooth muscle cells via blocking PDGF receptor and Erk-1/2. Int. J. Oncol. 29, 1247–1252. https://doi.org/10.3892/ijo.29.5.1247.
Peixoto, E.B., Papadimitriou, A., Teixeira, D.A.T., Montemurro, C., Duarte, D.A., Silva, K. C., Joazeiro, P.P., Lopes de Faria, J.M., Lopes de Faria, J.B., 2015. Reduced LRP6 expression and increase in the interaction of GSK3β with p53 contribute to podocyte apoptosis in diabetes mellitus and are prevented by green tea. J. Nutr. Biochem. 26, 416–430. https://doi.org/10.1016/j.jnutbio.2014.11.012.
Perva-Uzunalić, A., Škerget, M., Knez, Ž., Weinreich, B., Otto, F., Grüner, S., 2006. Extraction of active ingredients from green tea (Camellia sinensis): extraction efficiency of major catechins and caffeine. Food Chem. 96, 597–605. https://doi.org/10.1016/j.foodchem.2005.03.015.
Rachid, A., Rabah, D., Farid, L., Zohra, S.F., Houcine, B., 2012. Ethnopharmacological survey of medicinal plants used in the traditional treatment of diabetes mellitus in the North Western and South Western Algeria. J. Med. Plants Res. 6, 2041–2050. https://doi.org/10.5897/JMPR11.1796.
Rebhan, M., Chalifa-Caspi, V., Prilusky, J., Lancet, D., 1998. GeneCards: a novel functional genomics compendium with automated data mining and query reformulation support. Bioinformatics 14, 656–664. https://doi.org/10.1093/bioinformatics/14.8.656.
Renno, W.M., Abdeen, S., Alkhalaf, M., Asfar, S., 2008. Effect of greean tea on kidney tubules of diabetic rats. Br. J. Nutr. 100, 652–659. https://doi.org/10.1017/S0007114508911533.
Ribback, S., Cigliano, A., Kroeger, N., Pilo, M.G., Terracciano, L., Burchardt, M., Bannasch, P., Calvisi, D.F., Dombrowski, F., 2015. PI3K/AKT/mTOR pathway plays a major pathogenetic role in glycogen accumulation and tumor development in renal distal tubules of rats and men. Oncotarget 6, 13036–13048. https://doi.org/10.18632/oncotarget.3675.
Ricart-Jané, D., Llobera, M., López-Tejero, M.D., 2002. Anticoagulants and other preanalytical factors interfere in plasma nitrate/nitrite quantification by the Griess method. Nitric Oxide - Biol. Chem. 6, 178–185. https://doi.org/10.1006/niox.2001.0392.
Sartippour, M.R., Heber, D., Zhang, L., Beatty, P., Elashoff, D., Elashoff, R., Go, V.L., Brooks, M.N., 2002. Inhibition of fibroblast growth factors by green tea. Int. J. Oncol. 21, 487–491. https://doi.org/10.3892/ijo.21.3.487.
Scardoni, G., Petterlini, M., Laudanna, C., 2009. Analyzing biological network parameters with CentiScaPe. Bioinformatics 25, 2857–2859. https://doi.org/10.1093/bioinformatics/btp517.
Sertorio, M.N., Souza, A.C.F., Bastos, D.S.S., Santos, F.C., Ervilha, L.O.G., Fernandes, K. M., de Oliveira, L.L., Machado-Neves, M., 2019. Arsenic exposure intensifies glycogen nephrosis in diabetic rats. Environ. Sci. Pollut. Res. 26, 12459–12469. https://doi.org/10.1007/s11356-019-04597-1.
Shannon, P., 2003. Cytoscape: a software environment for integrated models of biomolecular interaction networks. Genome Res. 13, 2498–2504. https://doi.org/10.1101/gr.1239303.
Silva, M.J., Brodt, M.D., Lynch, M.A., McKenzie, J.A., Tanouye, K.M., Nyman, J.S., Wang, X., 2009. Type 1 diabetes in young rats leads to progressive trabecular bone loss, cessation of cortical bone growth, and diminished whole bone strength and fatigue life. J. Bone Miner. Res. 24, 1618–1627. https://doi.org/10.1359/jbmr.090316.
Soetan, K.O., Olaiya, C.O., Oyewole, O.E., 2010. The importance of mineral elements for humans , domestic animals and plants : a review. Afr. J. Food Sci. 4, 200–222.
Su, J., Ye, D., Gao, C., Huang, Q., Gui, D., 2020. Mechanism of progression of diabetic kidney disease mediated by podocyte mitochondrial injury. Mol. Biol. Rep. https://doi.org/10.1007/s11033-020-05749-0.
Suzuki, T., Fujikura, K., Higashiyama, T., Takata, K., 1997. DNA staining for fluorescence and laser confocal microscopy. J. Histochem. Cytochem. 45, 49–53. https://doi.org/10.1177/002215549704500107.
Szklarczyk, D., Morris, J.H., Cook, H., Kuhn, M., Wyder, S., Simonovic, M., Santos, A., Doncheva, N.T., Roth, A., Bork, P., Jensen, L.J., Von Mering, C., 2017. The STRING database in 2017: quality-controlled protein-protein association networks, made broadly accessible. Nucleic Acids Res. 45, D362–D368. https://doi.org/10.1093/nar/gkw937.
Szklarczyk, D., Santos, A., Von Mering, C., Jensen, L.J., Bork, P., Kuhn, M., 2016. STITCH 5: augmenting protein-chemical interaction networks with tissue and affinity data. Nucleic Acids Res. 44, D380–D384. https://doi.org/10.1093/nar/gkv1277.
Tachibana, H., Koga, K., Fujimura, Y., Yamada, K., 2004. A receptor for green tea polyphenol EGCG. Nat. Struct. Mol. Biol. 11, 380–381. https://doi.org/10.1038/nsmb743.
Vallon, V., Thomson, S.C., 2017. Targeting renal glucose reabsorption to treat hyperglycaemia: the pleiotropic effects of SGLT2 inhibition. Diabetologia 60, 215–225. https://doi.org/10.1007/s00125-016-4157-3.
Van Aller, G.S., Carson, J.D., Tang, W., Peng, H., Zhao, L., Copeland, R.A., Tummino, P. J., Luo, L., 2011. Epigallocatechin gallate (EGCG), a major component of green tea, is a dual phosphoinositide-3-kinase/mTOR inhibitor. Biochem. Biophys. Res. Commun. 406, 194–199. https://doi.org/10.1016/j.bbrc.2011.02.010.
Vaz, S.R., de Amorim, L.M.N., de Nascimento, P.V.F., Veloso, V.S.P., Nogueira, M.S., Castro, I.A., Mota, J.F., Botelho, P.B., 2018. Effects of green tea extract on oxidative stress and renal function in diabetic individuals: a randomized, double-blinded, controlled trial. J. Funct. Foods 46, 195–201. https://doi.org/10.1016/j.jff.2018.04.059.
Waltner-Law, M.E., Wang, X.L., Law, B.K., Hall, R.K., Nawano, M., Granner, D.K., 2002. Epigallocatechin gallate, a constituent of green tea, represses hepatic glucose production. J. Biol. Chem. 277, 34933–34940. https://doi.org/10.1074/jbc.M204672200.
Yamabe, N., Yokozawa, T., Oya, T., Kim, M., 2006. Therapeutic potential of (-)-Epigallocatechin 3- O -gallate on renal damage in diabetic nephropathy model rats. J. Pharmacol. Exp. Therapeut. 319, 228–236. https://doi.org/10.1124/jpet.106.107029.
Yang, X., Tomás-Barberán, F.A., 2019. Tea is a significant dietary source of ellagitannins and ellagic acid. J. Agric. Food Chem. 67, 5394–5404. https://doi.org/10.1021/acs.jafc.8b05010.
Yin, D.D., Luo, J.H., Zhao, Z.Y., Liao, Y.J., Li, Y., 2018. Tranilast prevents renal interstitial fibrosis by blocking mast cell infiltration in a rat model of diabetic kidney disease. Mol. Med. Rep. 17, 7356–7364. https://doi.org/10.3892/mmr.2018.8776.
Yokozawa, T., Noh, J.S., Park, C.H., 2012. Green tea polyphenols for the protection against renal damage caused by oxidative stress. Evidence-based Complement. Alternative Med. https://doi.org/10.1155/2012/845917, 2012.
Yoon, S.P., Maeng, Y.H., Hong, R., Lee, B.R., Kim, C.G., Kim, H.L., Chung, J.H., Shin, B. C., 2014. Protective effects of epigallocatechin gallate (EGCG) on streptozotocin-induced diabetic nephropathy in mice. Acta Histochem. 116, 1210–1215. https://doi.org/10.1016/j.acthis.2014.07.003.
Yoshimura, M., Watanabe, Y., Kasai, K., Yamakoshi, J., Koga, T., 2005. Inhibitory effect of an ellagic acid-rich pomegranate extract on tyrosinase activity and ultraviolet-induced pigmentation. Biosci. Biotechnol. Biochem. 69, 2368–2373. https://doi.org/10.1271/bbb.69.2368.
Youn, H.S., Lee, J.Y., Saitoh, S.I., Miyake, K., Kang, K.W., Choi, Y.J., Hwang, D.H., 2006. Suppression of MyD88- and TRIF-dependent signaling pathways of toll-like receptor by (-)-epigallocatechin-3-gallate, a polyphenol component of green tea. Biochem. Pharmacol. 72, 850–859. https://doi.org/10.1016/j.bcp.2006.06.021.
Yu, H., Kim, P.M., Sprecher, E., Trifonov, V., Gerstein, M., 2007. The importance of bottlenecks in protein networks: correlation with gene essentiality and expression dynamics. PLoS Comput. Biol. 3, 713–720. https://doi.org/10.1371/journal.pcbi.0030059.
Zhang, X., Guo, K., Xia, F., Zhao, X., Huang, Z., Niu, J., 2018. FGF23 C-tail improves diabetic nephropathy by attenuating renal fibrosis and inflammation. BMC Biotechnol. 18, 1–9. https://doi.org/10.1186/s12896-018-0449-7.